

Interplay between electronic and crystallographic instabilities in the low-dimensional ferroelectric $\text{CuInP}_2\text{Se}_6$

This article has been downloaded from IOPscience. Please scroll down to see the full text article.

2003 J. Phys.: Condens. Matter 15 595

(<http://iopscience.iop.org/0953-8984/15/3/323>)

View [the table of contents for this issue](#), or go to the [journal homepage](#) for more

Download details:

IP Address: 171.66.16.119

The article was downloaded on 19/05/2010 at 06:30

Please note that [terms and conditions apply](#).

Interplay between electronic and crystallographic instabilities in the low-dimensional ferroelectric $\text{CuInP}_2\text{Se}_6$

Y Fagot-Revurat¹, X Bourdon^{2,3}, F Bertran^{1,4}, V B Cajipe^{2,5} and D Malterre¹

¹ Laboratoire de Physique des Matériaux, CNRS UMR 7556, BP 239, 54506 Vandoeuvre-les-Nancy, France

² Institut des Matériaux Jean Rouxel, CNRS UMR 6502, BP 32229, 44322 Nantes, France

Received 18 September 2002

Published 13 January 2003

Online at stacks.iop.org/JPhysCM/15/595

Abstract

Temperature-dependent high-resolution ultra-violet photoemission spectroscopy (PES) measurements combined with tight-binding linear muffin-tin orbital (LMTO) atomic-sphere approximation (TB-LMTO-ASA) band-structure calculations are carried out to study the polar ordering in the low-dimensional ferroelectric $\text{CuInP}_2\text{Se}_6$. In the paraelectric phase, the energy-dependent PES spectra are in good agreement with our LMTO calculations. Below $T_c \approx 230$ K, evidence for a strong redistribution of the experimental density of occupied states (DOS) is given. The LMTO calculations, accounting for the off-centre position of Cu atoms in the low- T phase, allow us to interpret this behaviour in terms of a redistribution of the partial Cu 3d DOS. This strong interplay between electronic and crystallographic instabilities is analysed in the light of a second-order Jahn–Teller effect acting as the driving force of the ferroelectric transition.

1. Introduction

The great number of potential applications of ferroic materials in sensor technology (piezoelectricity, optoelectronics) has for many years motivated a great deal of research aimed at a better understanding of their properties [1]. Nevertheless, the first attempt to explain the microscopic origins of ferroelectricity in the well-known 3D oxide BaTiO_3 was made only recently; a strong Ti d/O 2p hybridization associated with a small distortion has been

³ Present address: Département de Relations Industrielles, Ecole Nationale Supérieure de Chimie de Rennes, Avenue General Leclerc, F-35700 Rennes, France.

⁴ Present address: LURE, Bâtiment 209d, Université Paris-Sud, BP 34, F-91898 Orsay, France.

⁵ Present address: NOVA RD, Incorporated, 1525 3rd Street, Suitec, Riverside, CA 92507, USA.

identified as a major component of the ferroelectricity in such materials [2]. In this paper, we focus on a new family of layered (2D) ferroic compounds CuMP_2X_6 ($M = \text{In}$ or Cr , $X = \text{S}$ or Se), giving us the opportunity to study ferroelectric properties in a low-dimensional system. As already observed in the past two decades in the case of the related compounds $\text{Sn}_2\text{P}_2\text{X}_6$ with 3D-type structures [3], a wide variety of ordered electric dipole states occur in these materials, depending on the chemical nature of the cation M and anion X . Ferrielectric and antiferroelectric phases were reported for CuInP_2S_6 and CuCrP_2S_6 respectively in 1993 [4, 5]. These compounds consist of lamellae defined by a sulfur framework, which provides octahedral voids for the metal cations (Cu , In , or Cr) and P-P pairs (figure 1). Each layer containing the CuInP_2X_6 entities is linked to each other layer by weak van der Waals interactions, forming a lamellar crystallographic structure with negligible transverse (along the c -axis) structural and electronic coupling. CuInP_2S_6 is the model compound of this family, and presents a well-defined first-order order–disorder phase transition (PT) at $T_c \approx 315$ K (monoclinic space group Cc to $C2/c$). The Cu(I) sublattice is polar below T_c and coexists with an In(III) sublattice of unequal and opposite polarity, leading to ferrielectricity with polarization normal to the layer (along the c -axis) [5, 6]. In the paraelectric phase, the Cu(I) probability density shows a twofold-symmetric shape relative to the centre of the octahedral CuS_6 group. This dynamic disorder has been modelled crystallographically by three types of partially filled copper site with large thermal factors: an off-centre and quasi-trigonal one, an almost central or octahedral one, and a nearly tetrahedral one in the interlayer space. The PT is triggered by the cooperative freezing of intersite copper motions. This cooperative dipolar behaviour is supposed to arise from the combined presence of:

- (i) a flexible polyhedral building block in the form of the ethane-like P_2S_6 group combined with a planar morphology that constrains the cations to undergo antiparallel displacements;
- (ii) an off-centring displacement caused by an electronic instability in the form of a second-order Jahn–Teller (SOJT) effect related to the d^{10} electronic configuration of the cations.

The coordination chemistry of $\text{Cu } d^{10}$ salts often exhibits small energy barriers separating different local bonding arrangements leading to unstable electronic configurations; in octahedral (or tetrahedral) symmetry the probability of finding a Cu atom in threefold coordination is high, typically leading to activated ionic conductivity through trigonal faces. A SOJT coupling, involving the localized d^{10} states forming the top of the valence band (VB) and the s – p states of the bottom of the conduction band (CB), is predicted to yield such an instability [7]. This has been clearly demonstrated for the Cu tetrahedral site in CuCl [8]. In CuInP_2S_6 , the observation of ionic conductivity along the c -axis and the possibility for Cu atoms to be in off-centred quasi-trigonal distorted sites even above T_c naturally led to an investigation of the role of the SOJT effect in such phenomena. Despite numerous studies, there is still a need to quantify the modifications of the electronic structure with respect to this polar ordering and its relation to the off-centred cationic shifts in the crystal.

Band-structure calculations, on the one hand, take into account the experimental crystallographic structure, and give access to the density of occupied states (DOS). Angle-integrated UV photoemission spectroscopy (PES), on the other hand, is a direct measurement of the one-electron excitation spectrum providing the experimental DOS in the case of negligible electronic correlations. The interplay between electronic and crystallographic instabilities should thus be revealed by comparing the findings from these two techniques. Unfortunately, the strong semiconductive (SC) gap in CuInP_2S_6 (≈ 2.8 eV [9]) prevents accurate PES measurements due to strong charging effects. Nevertheless, PES can be performed on the analogous Se-substituted compound, where the SC gap value decreases to about 1.8 eV at room T . $\text{CuInP}_2\text{Se}_6$, which has high- and low- T structures ($P\bar{3}1c$ and $P31c$ respectively;

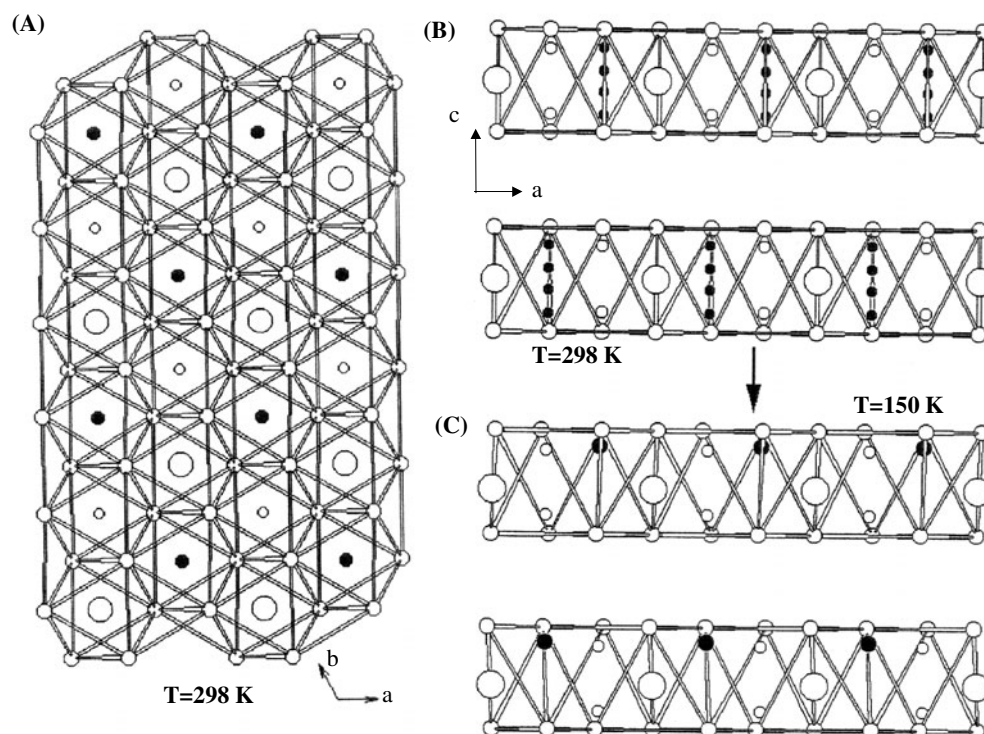


Figure 1. (A), (B) The $\text{CuInP}_2\text{Se}_6$ structure at $T = 298$ K (space group $P\bar{3}1c$, $a = b = 6.402$ Å, $c = 13.371$ Å); (C) an (a, c) view of $\text{CuInP}_2\text{Se}_6$ at $T = 150$ K. The small, medium, and large white circles represent P, Se, and In atoms respectively. The black circles, whose size is proportional to the occupation rate, represent Cu atoms.

figure 1) very similar to those of CuInP_2S_6 , is a relative newcomer in this class of materials and undergoes polar ordering below $T_c = 230$ K [10–12]. Dielectric measurements have recently confirmed the assumed paraelectric and ferroelectric characters of the high- and low- T phases, respectively [13]. This paper presents T -dependent PES measurements combined with LMTO band-structure calculations made for $\text{CuInP}_2\text{Se}_6$. Both the measured and the calculated DOS exhibit spectral changes around $T_c \approx 230$ K. These results are discussed in terms of cationic off-centring shifts possibly correlated with SOJT instability.

2. Experimental details

2.1. Photoemission measurements

Crystals of $\text{CuInP}_2\text{Se}_6$ were synthesized following the method described in [11]. The dark red crystals obtained were typically $5 \times 7 \times 0.5$ mm³ in size. PES measurements have been carried out on a Scienta SES-200 spectrometer with an energy resolution better than 10 meV. The base pressure in the photoemission chamber was 10^{-10} mbar. A He discharge lamp was used to produce photons of incident energies $h\nu = 21.8$ eV (He I mode) and 40.8 eV (He II mode). The crystals were fixed with silver epoxy to avoid charge effects and mounted on a He flux cryostat affording the possibility to perform PES in the range 20–350 K. Measurements on powder samples, scraped with a diamond file, were also made at room T . Measurements

were made for several cleavages and the PES spectra were found to be reproducible and strictly identical to those obtained for powder samples. The cleaved surface should be perpendicular to the c -axis due to the 2D structure and as observed for *ex situ* cleavage. However, its orientation should have no influence on the angle-integrated PES spectra. No surface contamination was observed during these experiments, confirming the chemical stability of this surface. The PES spectra were taken above and below T_c both in He I and He II modes, to check that there are no significant changes in PES spectra caused by changing the mean free path of the collected photoelectrons, as expected for a bulk-like transition.

2.2. Band-structure calculations

Scalar relativistic linearized tight-binding muffin-tin orbital calculations were performed within the atomic-sphere approximation (TB-LMTO-ASA calculations) using the LMTO47 program [15] with 20 atoms per hexagonal unit cell (2 fu). The space was filled with slightly overlapping Wigner–Seitz atomic spheres and additional empty spheres. The optimum radii and positions of these spheres were determined by using the method described in [16]; tables of the complete data used for the calculations are available from the authors. Convergence was obtained self-consistently using s, p, and d basis states at each atomic sphere with 384 k -points in the irreducible part of the Brillouin zone. We have used crystallographic results obtained at $T = 298$ and 150 K in [11]. At room T , we were not able to take into account the disorder observed on the Cu sites. The disorder has been modelled by introducing an average Cu position, i.e., the centre of the octahedral cage. This crude approximation should modify the electronic structure slightly, as we will see later. In order to facilitate comparison to PES experimental spectra, we have convoluted the calculated DOS with a Gaussian function with a FWHM equal to 300 meV.

3. Results and discussion

Figure 2 shows angle-integrated room T calculated total and partial densities of states (PDOS) for occupied and unoccupied states: He I and He II PES spectra (from the bottom to the top). Using the full theoretical DOS presented at the bottom of figure 2, we have simulated the theoretical He I and He II room T angle-integrated PES spectra, taking into account s, p, and d tabulated cross-sections [16] and the usual Shirley-type background. Calculations indicate that the low-energy part of the VB has mainly Cu 3d and Se 4p character (for $E_B < 5$ eV), whereas Se 4p, P 3p, and Cu 4s contribute to the first unoccupied states (the indium DOS is negligible and not presented here for clarity). We can identify seven peaks, with Cu 3d and Se 4p states with a substantial hybridization contributing to peak A, pure Cu 3d states to peak C, Se 4p states to peaks B and D, and hybridized Se 4p/P 3p states to peaks E, F, G. These seven peaks are clearly identified in the He I and He II experimental PES spectra. With increasing photon energy, cross-sectional effects lead to an enhancement of the d spectral features with respect to the s, p ones. Experimentally, the peaks A and C become dominant in the He II mode compared to peaks B and D in the He I spectrum. This is in good agreement with the calculated d character of peaks A and C and the p character of peaks B and D. The spectra are reproducible and do not change over time. Moreover, all spectral features present in our LMTO calculations are clearly identified by using two different incident energies and then two different probing depths, leading to the conclusion that the room T PES spectra are characteristic of bulk bands. Although the Fermi energy is exactly known in PES, it is difficult to refer to it for band-structure calculations in insulating compounds. Therefore, we decided to fix the Fermi energy of the calculated

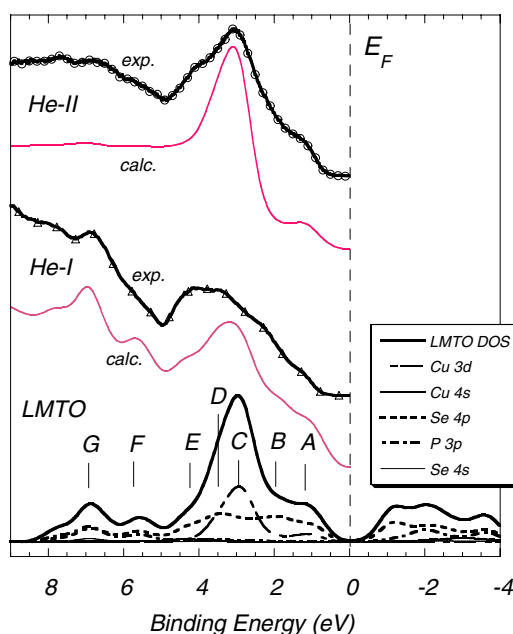


Figure 2. He II and He I calculated and measured PES spectra obtained at room temperature; LMTO partial and total DOS (see the explanation in the text).

(This figure is in colour only in the electronic version)

DOS by adjusting a maximum of the high-energy peaks (C, D, E, F, and G in figure 2) to experimental spectra. Thus, the experimental PES gap (≈ 1 eV) is substantially greater than the calculated one (≈ 0.6 eV). The full LMTO energy gap (≈ 1.2 eV) is also significantly smaller than the one determined from optical measurements (≈ 1.8 eV). A stronger PES gap value compared to the band-structure gap is usual and generally ascribed to correlation effects. In our case, this may also be understood in terms of a destabilization of the real electronic structure due to the average central position chosen for Cu atoms in the room T LMTO calculations.

PES experimental spectra obtained in the He II mode at $T = 300$ and 190 K are presented in figure 3. These spectra were found to be reproducible. They have been normalized to the spectral intensity at 5 eV. With decreasing T , low-energy Cu 3d levels have clearly shifted to higher binding energy (the peak A merges into the peak B) and the gap has slightly increased. We also observe strong changes at higher energy: the peak C at 3.3 eV decreases whereas the peak D at 3.7 eV increases. This substantial redistribution of low-energy spectral weights has also been evidenced in the He I mode in a separate experiment (not presented here), confirming that this effect cannot be attributed to surface effects (surface bands). The minor change in the optical gap ($< 5\%$) usually observed at the transition in CuInP_2X_6 is probably not enough to produce the charging effect at the transition. A charging effect (a shift of the entire spectrum) is only observed below $T \approx 150$ K and results from the very large increase in the resistivity with decreasing temperature, as expected for semiconducting materials at low T . This observation allows us to clearly separate the spectral redistribution due to the transition (around 230 K, well above 150 K) from the one caused by the temperature dependence of the resistivity (the charging effect below 150 K). The corresponding full DOS LMTO spectra calculated from the $T = 300$ and 150 K crystallographic structures are shown for comparison. The

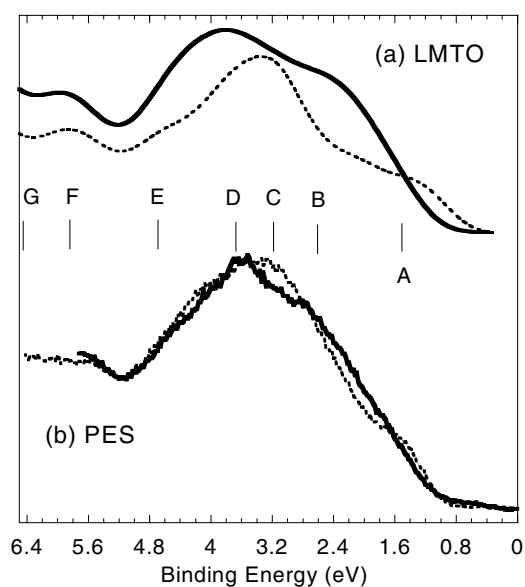


Figure 3. (a) The LMTO DOS obtained at $T = 298$ K (dashed curve) and $T = 150$ K (solid curve); (b) the corresponding PES spectra measured at $T = 298$ K (dashed curve) and $T = 190$ K (solid curve).

modifications as calculated and observed experimentally appear to be in fairly good agreement. Most of the changes observed in our PES spectra are at least qualitatively revealed in our band-structure calculations. This supports the conclusion that the redistribution of low-energy spectral weight observed in photoemission is strongly connected to crystallographic change, namely the octahedra distortion. These effects are more pronounced in the calculated DOS: the calculated energetic stabilization is probably amplified by the averaged Cu position being chosen to describe the paraelectric phase. We have decided to adjust the low- T calculated DOS so that the positions of the peaks B, C, and D above and below T_c in the calculations remain the same as experimentally determined. The only way to unambiguously adjust room T and low- T calculated spectra would be to perform total energy calculations, not available here. The pure Se 4p states (contributing mainly to peaks B and D) are not modified in a first approximation in our calculations and will not be discussed here. Cu 3d states, contributing to peaks A and C, are clearly modified below T_c . The calculated Cu 3d (occupied) and Cu 4s (unoccupied) PDOS are presented in figure 4 for $T = 300$ and 150 K. The intensity of the main structure (contributing to the experimental peak C) clearly decreases below T_c and the Cu PDOS is spread over a wide energy range, contributing also to other peaks (mostly peaks B and D). At the same time, the Cu 3d states giving rise to peak A above T_c are split into two contributions below T_c (figure 4), extending to the wide p, d block states at higher binding energy. This behaviour is observed experimentally. It is thus natural to attribute the low-energy DOS changes observed below T_c mainly to the Cu PDOS modifications associated with the off-centred position of copper atoms in the crystal (taken into account by our LMTO calculations).

We shall now discuss such DOS modifications in the light of the SOJT instability associated with the d^{10} copper electronic configuration in octahedral symmetry [7]. The lower-energy occupied levels for d^{10} ions in octahedral symmetry are formed by the two degenerate e_g orbitals (with $3d_{x^2-y^2}$ and $3d_{z^2}$ symmetries). In some cases, a hybridization between the filled nd Cu orbitals and the unoccupied $(n + 1)s$ orbitals leads to a energetically more favourable

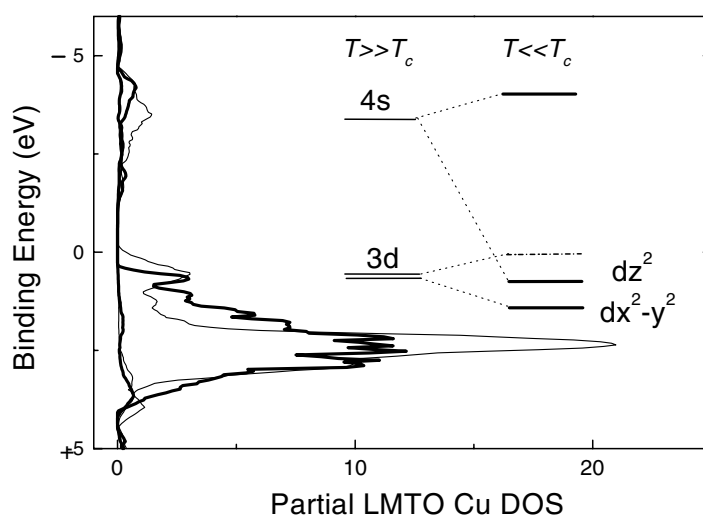


Figure 4. The Cu PDOS at $T = 298$ and 150 K versus energy diagram, illustrating the SOJT mechanism.

fundamental state associated with a distorted environment (from an octahedral to a quasi-trigonal site) leading to the SOJT distortion [8]. The twofold-degenerate levels are split, the $3d_{z^2}$ orbital is destabilized, and $3d_{x^2-y^2}$ is stabilized. The final energetic gain comes from the Cu $3d_{z^2}$ /Cu $4s$ hybridization leading to a stabilization of the $3d_{z^2}$ orbital and a destabilization of the Cu $4s$ orbitals [7]. Unfortunately, our LMTO calculations do not allow us to determine the symmetry of the energy levels. Nevertheless, the splitting of peak A into two contributions is exhibited clearly in the calculated Cu PDOS (figure 4). The new binding energy for the last occupied states (assumed to be the $3d_{z^2}$ orbital) is higher, consistent with a SOJT effect accompanied by a substantial energetic gain (around 0.3 eV). This is corroborated by the simultaneous increase in the binding energy of the unoccupied Cu $4s$ states observed in our LMTO calculations for $T \ll T_c$ (figure 4).

4. Summary and conclusions

Through PES measurements we have given evidence for a strong redistribution of the density of states at the top of the valence band observed for at least two different incident energies. By combining these with LMTO band-structure calculations, we have shown that these changes are mainly ascribable in the redistribution of the Cu PDOS, related to the off-centred position of the d^{10} cations in the ferrielectric phase. To our knowledge, we have presented here for the first time spectroscopic evidence for a strong interplay between crystallographic and electronic instabilities consistent with a SOJT effect as a major cause of the cooperative dipolar ordering in a ferroelectric material. No SOJT effect was observed for the In(III) d^{10} cation, as could be expected because its d^{10} orbitals are too low in energy. The In off-centring shifts may then be attributed to a relaxation effect, related to the order–disorder transition type in CuInP_2S_6 in which no displacive component associated with In(III) has so far been observed [17].

The mechanisms of the transition in $\text{CuInP}_2\text{Se}_6$ still merit detailed study. We can assume that they are close to those of CuInP_2S_6 . One striking point that needs to be mentioned here is the recent discovery of an intermediate phase (IC) in $\text{CuInP}_2(\text{S}_{1-x}\text{Se}_x)_6$

for $T_c = 236 \text{ K} < T < T_I = 248 \text{ K}$ and $x = 1$. The high- T paraelectric and low- T ferroelectric phases are separated for $x > 0.28$ by two successive transitions: a second-order one at T_{IC} and a first-order one at T_c separated by an incommensurate phase [13]. These two transition lines merge into just one for $x \approx 0.28$, this point being a possible Lifshitz point. Despite the presence of this peculiar IC phase in $\text{CuInP}_2\text{Se}_6$, we believe that our results, obtained well above and below T_c , can be extended to CuInP_2S_6 . Our first LMTO calculations for this system tend to confirm this hypothesis. Moreover, there is evidence for an IC phase in the related 3D system $\text{Sn}_2\text{P}_2(\text{Se}_x\text{S}_{1-x})_6$, where the transition mechanisms remain similar for $x = 0$ and 1 (despite the presence of the IC phase). Nevertheless, the driving force, mainly attributed to the lone free electron pair of the Sn(II), would be very different compared to that of CuInP_2S_6 [18]. These findings and seeming similarities between these 2D and 3D ferroelectrics suggest a possibly important role of the P_2X_6 entity in enabling dipole ordering in these materials. A careful examination of these aspects by means of LMTO and total energy calculations, for both CuInP_2X_6 and $\text{Sn}_2\text{P}_2\text{X}_6$, will be carried out.

Acknowledgment

We would like to acknowledge Professor Y M Vysochanskii for helpful discussions.

References

- [1] Auciello O, Scott J F and Ramesh R 1998 *Phys. Today* **July**
- [2] Zhong W, Vanderbilt D and Rabe K M 1994 *Phys. Rev. Lett.* **73** 1861
Cohen R E 1992 *Nature* **358** 136
- [3] Vysochanskii Y M and Slivka V Y 1992 *Sov. Phys.-Usp.* **35** 123
Eijt S W-H, Currat R, Lorenzo J E, Saint Gregoire P, Katano S, Janssen T and Hennion B 1998 *J. Phys.: Condens. Matter* **10** 4811 and references therein
- [4] Maisonneuve V, Payen C and Cajipe V B 1993 *Chem. Mater.* **5** 758
- [5] Maisonneuve V, Cajipe V B, Simon A, Von Der Muhll R and Ravez J 1997 *Phys. Rev. B* **56** 10860 and references therein
- [6] Bourdon X, Grimmer A R and Cajipe V B 1999 *Chem. Mater.* **11** 2680
- [7] Burdett J K and Eisenstein O 1992 *Inorg. Chem.* **31** 1758
- [8] Wei S H, Zhang S and Zunger A 1993 *Phys. Rev. Lett.* **70** 1639
- [9] Studenyak I P, Mytrovcij V V, Kovacs G S, Gurzan M I, Mykajlo O A, Vysochanskii Y M, Cajipe V B and Bourdon X *Preprint*
- [10] Bourdon X, Maisonneuve V, Cajipe V B, Payen C and Fisher J E 1999 *J. Alloys Compounds* **283** 122
- [11] Bourdon X 1999 *PhD Thesis* University of Nantes, France
- [12] Bourdon X, Maisonneuve V and Cajipe V J 2003 in preparation
- [13] Vysochanskii Y M, Molnar A A, Gurzan M I, Cajipe V B and Bourdon X 2000 *Solid State Commun.* **115** 13
- [14] Andersen O K and Jepsen O 1984 *Phys. Rev. Lett.* **53** 2571
- [15] Jepsen O and Andersen O K 1995 *Phys. Rev. B* **35** 97
- [16] Yeh J J and Lindau I 1985 *At. Data Nucl. Data Tables* **32** 1
- [17] Vysochanskii Y M, Stephanovich V A, Molnar A A, Cajipe V B and Bourdon X 1998 *Phys. Rev. B* **58** 9119
- [18] Scott B, Pressprich P, Willet R D and Clearly D A 1992 *J. Solid State Chem.* **96** 294